



# The effects of surface roughness and nanostructure on the properties of indium tin oxide (ITO) designated for novel optoelectronic devices fabrication

G. Kavei\*, A. Mohammadi Gheidari

Material & Energy Research Center (MERC), P.O. Box 14155-4777, Tehran, Iran

## ARTICLE INFO

### Article history:

Received 14 August 2007

Received in revised form

1 January 2008

Accepted 13 January 2008

### Keywords:

Scanning probe microscopy (SPM)

Atomic force microscopy (AFM)

Q quality factor

Surface roughness

## ABSTRACT

Indium tin oxide (ITO) was deposited on a glass (Soda Lime glass) by RF sputtering system at different sputtering gas (Argon/oxygen 90/10%) pressures (20–34 mTorr) at room temperature. The sputtering rate was depended on sputtering gas pressure. The optimum sputtering gas pressure of 27 mTorr provides homogenous and most favorable rate of deposition. The samples at different thicknesses (168, 300, 400, 425, 475, 500 and 630 nm) were deposited on substrate and were annealed at 350, 400 and 450 °C to evaluate annealing process effects on the involved parameters. Structures, transparency, electrical conductivity and surface roughness of the films were characterized before and after annealing process. Surface properties were measured by scanning probe microscopy (SPM) in contact atomic force mode and the effect of thermal annealing on roughness of the surface and on the structure of deposited film was investigated. The films will exhibit considerable ratio of the optical transmittance to the electrical conductivity. A criterion factor,  $Q$ , is defined as the ratio of the normalized average transmittance to normalized resistivity. In addition to intrinsic parameters of ITO,  $Q$  severely depends on surface roughness.

© 2008 Elsevier B.V. All rights reserved.

## 1. Introduction

Transparent conductors were of interest to scientists since 1907, when reports of transparent and conductive cadmium oxide (CdO) films first published. Since then there has been a growing technological interest in materials with these unique properties as evidenced by not only their increased numbers but also the large variety of techniques that have been developed for their deposition. It is now known that non-stoichiometric and doped films of oxides of tin, indium, cadmium, zinc and their various alloys exhibit high transmittance and nearly metallic conductivity (Chopra et al., 1983).

Although partial transparency, with rational reduction in conductivity, can be obtained for many thin metallic films,

high transparency and high conductivity cannot be attained simultaneously in intrinsic stoichiometric materials. The only way is to create electron degeneracy in a wide band-gap material ( $E_g > 3$  eV or more for visible radiation) by controllably introducing non-stoichiometry and/or appropriate dopants. These conditions can be conveniently met for ITO as well as a few other materials mentioned above (Nath and Bunshah, 1980).

Nowadays, the technology of optical sensors and solar cells is being more and more important (Bätzner et al., 2000; Terzini et al., 1999, 2000; Guillen and Herrero, 2006; Kerkach et al., 2006). Indium tin oxide (ITO), deposited on a transparent glass, has many advantages for sensors and solar cells including good mechanical and optical properties. It is also a

\* Corresponding author. Tel.: +98 21 88771626; fax: +98 21 88773352.

E-mail addresses: [g-kavei@merc.ac.ir](mailto:g-kavei@merc.ac.ir), [ghassem113@yahoo.com](mailto:ghassem113@yahoo.com) (G. Kavei).  
0924-0136/\$ – see front matter © 2008 Elsevier B.V. All rights reserved.  
doi:10.1016/j.jmatprotec.2008.01.024

good electrical insulator and can be bonded easily to silicon substrates at room temperature (lower than the temperature needed for fusion bonding).

However, tin doped indium oxide (ITO) with reported transmittance and conductivity as high as 5% and  $10^4 (\Omega \text{ cm})^{-1}$ , respectively, is most popular material for electronic, optoelectronic and mechanical applications.

Indium tin oxide is essentially formed by substitutional doping of  $\text{In}_2\text{O}_3$  with Sn which replaces  $\text{In}^{3+}$  atoms from cubic bixbyite structure of indium oxide (Fan and Goodenough, 1977). ITO films have lattice parameter close to that of  $\text{In}_2\text{O}_3$  which lies within the range of 10.2–10.31 Å (Nath and Bunshah, 1980). Thus, Sn forms an interstitial bond with oxygen either at SnO or  $\text{SnO}_2$  forms, with a valence of +2 or +4, respectively. This valence state plays an important role in conductivity of ITO. The lower valence state results in reduction in carrier conductivity. When a hole is created, it acts as a trap and reduces conductivity. Existence of the  $\text{SnO}_2$  state means existence of  $\text{Sn}^{4+}$ , which implies that  $\text{SnO}_2$  acts as an n-type donor. However, in ITO, both substituted tin and oxygen vacancies result in high conductivity, and the formula of the compound is represented as  $\text{In}_{2-x}\text{Sn}_x\text{O}_{3-2x}$ .

There are different ways to enhance the efficiency of some optical devices such as solar cells, sensors, etc. In one of these methods light is allowed to have more reaction with material by roughening the surface. Reliable roughness is obtained by annealing the sample. Hence, surface characterization plays an important role. In recent years, atomic force microscopy (AFM) has become a valuable system to measure and discern the surface properties such as roughness, electrical and magnetic parameters of materials in small scales (Bruce, 1997; Barabasi and Stanley, 1995; Jafari et al., 2003). Since wave scattering depends on the morphology of rough surfaces, it is an important parameter on ITO films, in particular when used as solar cells. A summary of electrical and optical properties of typical ITO films deposited using various techniques is reported by Bashar (1997).

## 2. Experimental

### 2.1. Material preparation

A commercial type of ITO which is a ceramic disc with ( $\text{In}_2\text{O}_3/\text{SnO}_2$ : 90/10%) formula, was placed as target of sputtering and a cleaned glass (Soda Lime glass) as a substrate. System was evacuated up to  $\sim 10^{-5}$  Torr before sputtering. For all deposition steps the target was pre-sputtered for 15 min in the selected sputtering condition to warranty the purity of ITO deposited on the substrate. To make plasma medium for sputtering (Argon/oxygen: 90/10%) gas was admitted into the system, increasing vacuum pressure to  $\sim 10^{-3}$  Torr. Indium tin oxide was deposited on a glass by RF sputtering system at different sputtering gas pressures (20–34 mTorr) at room temperature. For all samples, the deposited films were kept at different sputtering gas pressures at 60 min to have different thicknesses. Layers with various thicknesses (168, 300, 400, 425, 475, 500 and 630 nm) were obtained. Plasma of the mixed gas collided to the target by a rate of  $10^{-3} \text{ cm}^3/\text{min}$  at voltage of 10 kV and the measured sputtering power of 350 W, deposit-

ing the ITO on the glass substrate (Soda Lime glass which can tolerate a temperature as high as  $500^\circ\text{C}$ ). Surface resistance and light transmission properties were measured by four point probes and a double beam PerkinElmer spectrophotometer, respectively, as by Mohammadi Gheidari et al. (2007).

### 2.2. AFM and XRD observations

Atomic force microscopy characterizes the profile of surface morphology and its nanostructure precisely (Bruce, 1997; Barabasi and Stanley, 1995; Jafari et al., 2003). In “Contact Atomic Force Microscopy” (C-AFM), which is suitable for ordinary samples, the tip-sample contact area is minima, providing the highest resolution (sub-nanometer) in imaging of stochastic topographical features. The height on the images (z), recorded in C-AFM, also represents the most accurate, true topography of the samples. For non-destructive imaging and convoluted features of the samples, force interaction between the C-AFM tip and the sample surface must be minimized. This is done by means of selecting an appropriate tip depending on the degree of the surface roughness and hardness of the sample. Provided tip for AFM imaging prevents surface damage by eliminating the lateral forces that are inherent in contact mode (where the tip is simply dragged over the surfaces).

The AFM used in this study was Solver Pro (NT-MDT Ltd., Moscow, Russia) operating in C-AFM mode. The tips used were CG01S, compatible with most of SPM devices with nominal force constant  $0.03 \text{ N m}^{-1}$ . Images were manipulated using Flatten 2nd order processing software. To record AFM images, samples were fixed carefully on the sample holder by two side adhesive Selo tape.

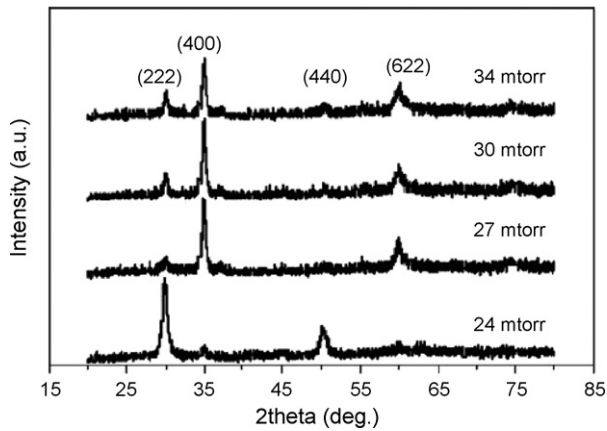
The microstructural properties of the sample were investigated by X-ray diffraction (XRD). The conventional X-ray diffractometer using Philips (30 kV, 20 mA) diffractometer with  $\text{Cu-K}\alpha$  radiation ( $\lambda = 1.54056 \text{ \AA}$ ) have been employed for analyzing the properties of the films at room and annealed temperatures.

Samples were kept under the pressure of  $10^{-5}$  Torr at room temperature, then gently warmed up to 200, 300, 350, 380, 400 and  $450^\circ\text{C}$  at a vacuum of  $10^{-5}$ – $10^{-4}$  Torr. In order to realize the post-annealing effect on the physical, structural and electro-optical properties of the films, these properties were studied by means of the XRD, SPM, spectrophotometer and four point probe technique once more. Some physical properties of the films were also taken from the XRD and transmission data.

## 3. Results and discussions

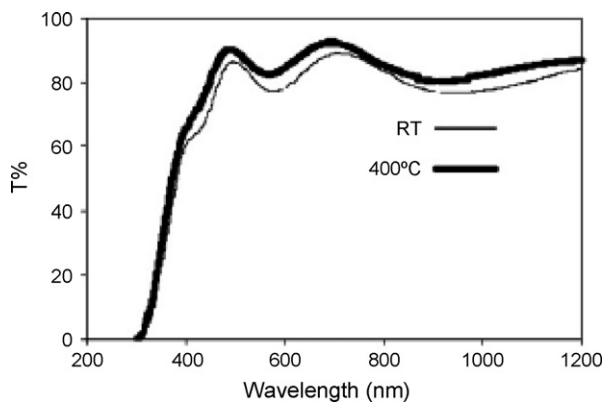
### 3.1. Deposited samples

Fig. 1 shows the XRD analysis of the some selected samples prepared at sputtering gas pressures of 24, 27, 30 and 34 mTorr at a sputtering power of 350 W with deposition time of 60 min. All samples were annealed up to  $400^\circ\text{C}$ . In this figure, the main growth planes are (2 2 2), (4 0 0), (4 4 0) and (6 2 2), which are related to the cubic structure of  $\text{In}_2\text{O}_3$  as reported by Hu et al. (2004). It is also quoted by Terzini et al. (2000) that for



**Fig. 1 – XRD analysis of ITO films prepared at sputtering gas pressure of 24, 27, 30 and 34 mTorr, at 400 °C.**

the films deposited at sputtering pressures of 20–24 mTorr and 400 °C, the ratio of the intensity of (222) peak to that of (400), i.e. ( $I_{222}/I_{400}$ ) is 5 times (or even more) the standard value of this ratio for ITO powder. Therefore, the most part of the layer parallel to surface has been textured in (111) direction, while for films deposited at sputtering pressure of 27–34 mTorr this ratio is much less than standard value, resulting higher intensity in the (100) direction textured films. Many authors have studied the crystal growth orientation and texture of just deposited films. It is commonly believed that the plasma density changes with sputtering pressure and sputtering power. The change in the plasma density during the deposition of ITO films alters the film properties by influencing the thermalization distance (Vassant Kumar and Mansingh, 1989; Terzini et al., 1999). When the thermalization distance is larger than target to substrate distance, an energetic impingement of  $O^-$  ions with growing surface leads to oxygen deficient films (films prepared at sputtering gas pressure of 27–34 mTorr), which tend to orient along (400) direction, while for low sputtering pressure of 20–24 mTorr, the thermalization distance is smaller than target to substrate gap, therefore the films have more reduced oxygen vacancies and tend to grow in (222) direction (Terzini et al., 2000; Aggour et al., 2000; Guillen and Herrero, 2003).



**Fig. 2 – Transmittance spectra for 27 mTorr just deposited (room temperature) and 400 °C annealed films.**

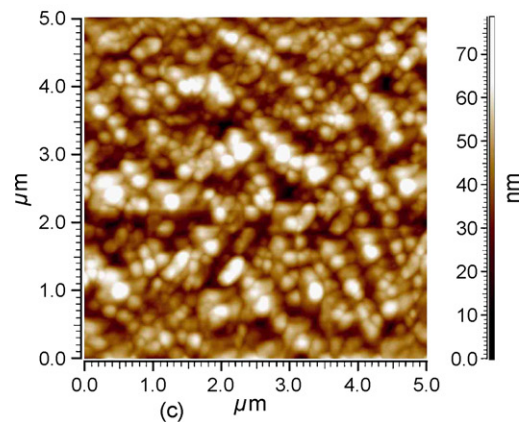
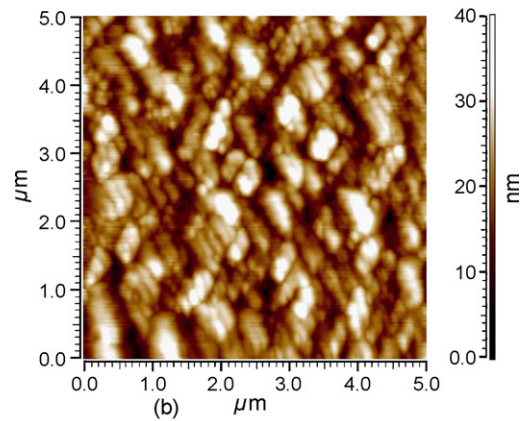
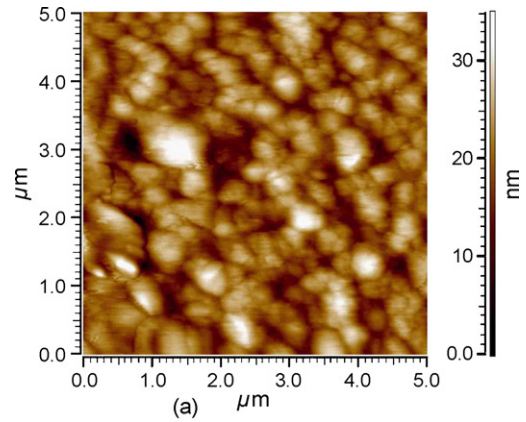


**Fig. 3 – The surface roughness against film thicknesses: (a) 425 nm 2D image; (b) 475 nm 2D image; (c) 630 nm 2D image; at room temperature. The thicker film has rough surface.**

The lattice parameters for different sputtering gas pressure (calculated from XRD strongest peak) and interplanar distances ( $d$ ) of the film at room temperature are summarized by Mohammadi Gheidari et al. (2007). It was concluded that as film growth is in progress, the films are under tensile stress. For the films prepared at high sputtering power and room temperature, the larger value of lattice parameter can fairly be attributed to the introduction of Sn atoms into the crystal lattice (Kerkach et al., 2006). The lattice parameters and plane distances decrease with sputtering pressure increment

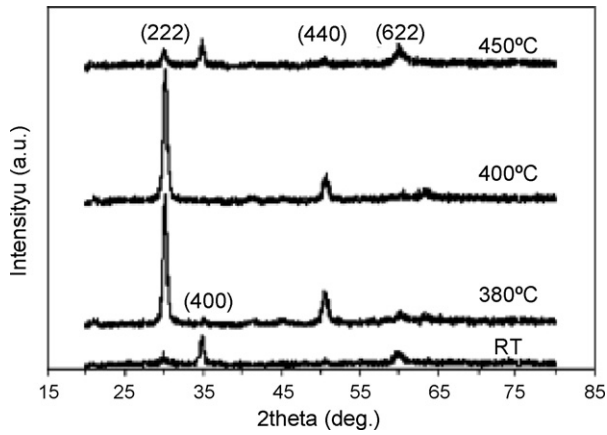
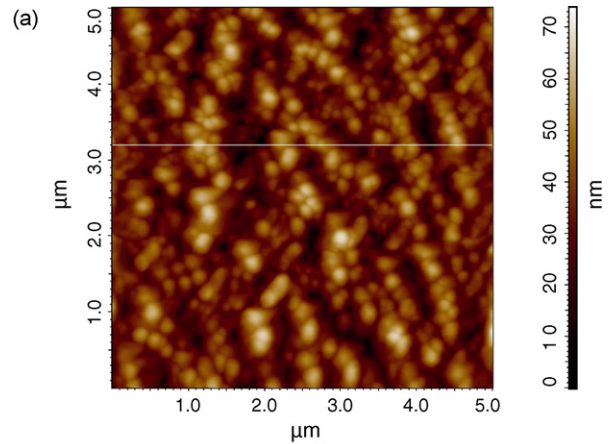


**Fig. 4 – XRD analysis of the films with 300 nm thickness and sputtering gas pressure of 27 mTorr at room temperature and annealed at 380, 400 and 450 °C.**

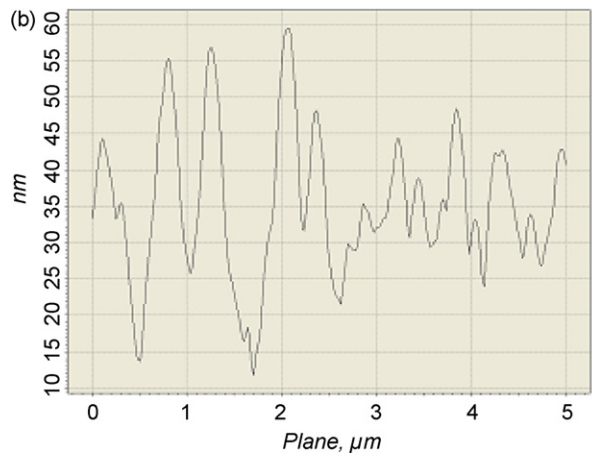
from 24 to 30 mTorr. This is attributed to higher oxygen vacancies at higher sputtering pressure and anti-site defects in the structure (Horák et al., 2007).

Fig. 2 shows the measured transmittance of a typical ITO film over the wavelength range of 200–1200 nm. The films were deposited at 27 mTorr sputtering gas pressure. One can see that within the range of 450–1200 nm of the wavelength (corresponding to 2.76–1.03 eV energy range) transmittance exceeds 80% which covers the majority of the III–V compound semiconductors such as AlAs, AlGaAs, GaAs, InP and InGaAs as well as Si and Ge. Energy gap fluctuations for the films deposited at sputtering gas pressure of 24–30 mTorr is attributed to the structure, roughness variation and increasing oxygen vacancy (Terzini et al., 2000; Kerkach et al., 2006).

In depositing a film as a layer, for instance, decreasing the thickness of layer weakens electrical properties, while increasing the thickness of layer makes it opaque. During deposition, structures of matter and colorant can be modified. Roughness of deposited layer and colorant may profusely affect reflection or transmission factor. However, thicker films have high electrical conductivity; this is well supported by film’s resistivity variation (Barabasi and Stanley, 1995), and rough surface as discussed by Jafari et al. (2007). Fig. 3 shows some selected images of samples with different thickness. This figure and the following figures show the effect of thickness and roughness on the optical and electrical properties and as a result on factor.



Peak-to-peak, $S_y$	71.0981 nm
Ten point height, $S_z$	35.3377 nm
Average	35.1687 nm
Average Roughness, $S_a$	8.75594 nm
Second moment	36.8031
Root Mean Square, $S_q$	10.8456 nm



**Fig. 5 – (a) 2D image and statistical values of the recorded image of the just deposited sample (not annealed), and (b) fluctuations of the surface structure in a direction parallel to the x axis along the line shown on (a).**

**Table 1 – The relative intensity of the (222)/(400), interplaner distances, average optical surface resistivity and transmission of the films in various annealing temperatures**

No.	Annealing temperature (°C)	(222) intensity relative to (400)	Interplaner distances, $d$ (Å)	Surface resistivity ( $\Omega$ cm <sup>2</sup> )	Average transmission (%)
1	Room	Amorphous	Amorphous	1k	84
2	200	0.14	2.982	301	83
3	300	0.51	2.980	89	80
4	400	1	2.954	17	86
5	450	0.66	2.961	45	86

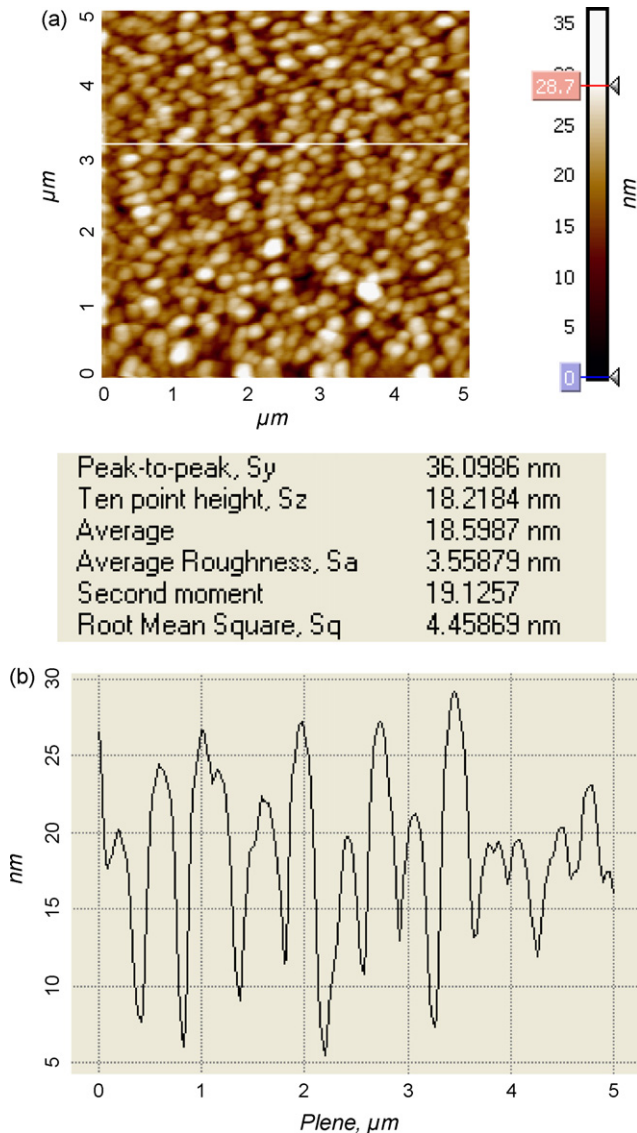


**Fig. 6 – (a) 2D image and statistical values of the recorded image of the annealed sample tested in Fig. 5, and (b) fluctuations of the surface structure in a direction parallel to the x axis along the line shown on (a).**

### 3.2. Annealed samples

Fig. 4 shows the XRD spectra of some selected samples prepared with 300 nm thickness and sputtering gas pressure of 27 mTorr at room temperature, 380, 400 and 450 °C, respectively. In this figure, the variation of the (222) and (400) peak intensities for the films versus annealing temperature are demonstrated. The (400) peak disappears with increment of annealing temperature up to 400 °C and reappears at 450 °C, while the intensity of (222) peak behaves inversely. Similarly, Holmelund et al. (2002) observed a strongly preferred [111] direction textured film deposited at substrate temperature of 200 °C by pulsed laser deposition technique. Therefore the temperature of 400 °C is most suitable annealing temperature for our samples. The variation of (222) and (400) crystallites sizes (from XRD data), lattice param-

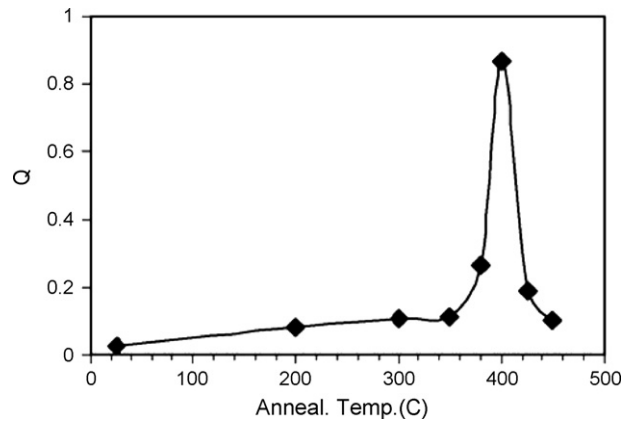


**Fig. 7 – Variation of the Q value vs. annealing temperature.**

eter and interplaner distance ( $d$ ) for (222) and (400) crystal planes are presented in Table 1. The (400) oriented crystallites are larger in intensity than (222). Such films have a scattered nature depending on annealing temperature. The size of (222) crystallites increases with increment of annealing temperature and takes the maximum value of 26.2 nm at 400 °C. The interplaner distance,  $d$ , for (222) crystal planes decreases systematically with increment of temperature to 400 °C. This means that film favors to release its stress along [111] direction during annealing and at 400 °C it has minimum value of stress. The relative intensity of the (222)/(400), interplaner distances, average optical surface resistivity and transmission of the films in various annealing temperatures are summarized in Table 1. The surface resistivity of the films takes its lowest value at 400 °C along with transmission enhancement; which is attributed to larger carrier mobility, film crystallite improvement and grain size enlargement at this temperature (Barabasi and Stanley, 1995; Jafari et al., 2003; Bashar, 1997; Mohammadi Gheidari et al., 2007; Hu et al., 2004; Vassant Kumar and Mansingh, 1989; Aggour et al., 2000).

Effect of the surface roughness of the films on optical and electrical properties were studied and the properties related to the fluctuations on the surface of unprocessed and annealed films were compared using SPM images. Fig. 5(a) shows the AFM 2D image of the sample with thickness of 630 nm with no thermal process on the sample, roughness data recorded shown in Fig. 5(a) and the profile of the fluctuations on the surface is given in Fig. 5(b) along the line in Fig. 5(a) to give a high prospectus from the surface. Fine grains appeared on the surface probably were associated with ITO and much closed boundary grains. Fig. 6 illustrates images of the same sample after thermal operation in which sample was heated to 400 °C (definitions of the figure are as for Fig. 5). Thermal modification enlarged boundary grains (which can be clearly seen in the image) and results in improved optical properties. This is clear in Fig. 2 where, the optical transmission spectra of visible and near-IR spectrum for just deposited films annealed at 400 °C are shown. Figs. 5 and 6 shows that the films have a granular structure the grain sizes and shapes in these images (35–40 nm) are larger than those calculated from XRD spectra (26.2 nm).

However, in optical systems, fraction of reflected or transmitted light is to be measured. This implies that the substance should have optimum values for both electrical conductivity and light transmission. The quality of the system is defined by criterion parameter  $Q$ , which characterizes the electro-optical properties of the films; that is the ratio of normalized average transmission to normalized resistivity. Nevertheless, this factor is severely affected by surface roughness (Bruce, 1997). In this study, the average transmission and surface resistivity of the films have been normalized to 90% and  $2 \times 10^{-4} \Omega \text{ cm}^2$ , respectively. The variation of  $Q$  with temperature is shown in Fig. 7. The maximum value of  $Q$  is obtained at  $400^\circ\text{C}$ .

#### 4. Conclusions

ITO thin films have been deposited onto Soda Lime glass substrates by RF sputtering at different sputtering gas pressures (20–34 mTorr). The deposition rate increased by increment of the sputtering gas pressure up to 30 mTorr and decreased above 30 mTorr. The films crystal orientation changed from [111] to [100] as the sputtering gas pressure exceeded 24 mTorr. The sputtering gas pressure of 27 mTorr, leading to good combined electrical conductivity and optical transparency, was used to deposit the films and these films were annealed at different temperatures in vacuum. Surface roughness study revealed that the grains were well arranged at  $400^\circ\text{C}$  and therefore had lowest scattering coefficient. However, the annealing temperature of  $400^\circ\text{C}$  lead to better conductivity and transparency, larger grain size and lower stress for the films. The criterion parameter  $Q$  is defined as the films figure-of-merit. Maximum value for  $Q$  was obtained at  $400^\circ\text{C}$ , too. It also evaluates the quality of material for solar cell and optical sensors application.

#### REFERENCES

- Aggour, M., Lewerenz, H.J., Klaer, J., Störkel, U., 2000. Electrochemical processing of surface layers on  $\text{CuInS}_2$  thin film solar cell absorbers. *Electrochem. Solid-State Lett.* 3, 399–402.
- Barabasi, A.L., Stanley, H.E., 1995. *Fractal Concepts in Surface Growth*. Cambridge University Press, New York.
- Bashar S.A., 1997. Thesis, “Study of indium tin oxide (ITO) for novel optoelectronic devices”. University of London Regulations for the Degrees of M.Phil. and Ph.D. (October).
- Bätzner, D.L., Öszan, M.E., Bonnet, D., Bücher, K., 2000. Device analysis methods for physical cell parameters of CdTe/Cds solar cells. *Thin Solid Films* 361–362, 547.
- Bruce, N.C., 1997. Scattering of light from surfaces with one-dimensional structure calculated by the ray-tracing method. *J. Opt. Soc. Am. A* 14, 1850–1858.
- Chopra, K.L., Major, S., Pandya, D.K., 1983. Transparent conductors—a status review. *Thin Solid Films* 102, 1–46.
- Fan, J.C.C., Goodenough, J.B., 1977. X-ray photoemission spectroscopy studies of Sn-doped indium oxide films. *J. Appl. Phys.* 48 (8), 3524–3531.
- Guillen, C., Herrero, J., 2003. Electrical contacts on polyimide substrates for flexible thin film photovoltaic devices. *Thin Solid Films* 431–432, 403.
- Guillen, C., Herrero, J., 2006. Polycrystalline growth and recrystallization processes in sputtered ITO thin films. *Thin Solid Films* 510, 260.
- Holmelund, E., Thestrup, B., Larsen, N.B., Nielsen, M.M., Johnson, E., Tougaard, S., 2002. Deposition and characterization of ITO films produced by laser ablation at 355 nm. *Appl. Phys. A (Mater. Sci. Process.)* 74, 147.
- Horák, J., Lošták, P., Drasa, Č., Navra, J., Uherc, C., 2007. Defect structure of  $\text{Sb}_{2-x}\text{Fe}_x\text{Te}_3$  single crystals. *J. Solid State Chem.* 180, 915–921.
- Hu, Y., Diao, X., Wang, C., Hao, W., Wang, T., 2004. Effects of heat treatment on properties of ITO films prepared by RF magnetron sputtering. *Vacuum* 75, 183.
- Jafari, G.R., Fazeli, S.M., Ghasemi, F., Vaez Allaei, S.M., Rahimi Tabar, M.R., Irajizad, A., Kavei, G., 2003. Etched glass surfaces, atomic force microscopy and stochastic analysis. *Phys. Rev. Lett.* 91, 226101.
- Jafari, G.R., Rahimi Tabar, M.R., Irajizad, A., Kavei, G., 2007. Etched glass surfaces, atomic force microscopy and stochastic analysis. *Physica A* 375, 239–246.
- Kerkach, L., Layadi, A., Dogheche, E., Remiens, D., 2006. Physical properties of RF sputtered ITO thin films and annealing effect. *J. Phys. D: Appl. Phys.* 39, 184–189.
- Mohammadi Gheidari, A., Behafarid, F., Kavei, G., Kazemzad, M., 2007. Effect of sputtering pressure and annealing temperature on the properties of indium tin oxide thin films. *Mater. Sci. Eng. B* 136, 37–40.
- Nath, P., Bunshah, R.F., 1980. Preparation of  $\text{In}_2\text{O}_3$  and tin-doped  $\text{In}_2\text{O}_3$  films by a novel activated reactive evaporation technique. *Thin Solid Films* 69, 63–68.
- Terzini, E., Nobile, G., Loreti, S., Minarini, C., Polichetti, T., Thilakan, P., 1999. Influences of sputtering power and substrate temperature on the properties of RF magnetron sputtered indium tin oxide thin films. *Jpn. J. Appl. Phys.* 38, 3448.
- Terzini, E., Thilakan, P., Minarini, C., 2000. Properties of ITO thin films deposited by RF magnetron sputtering at elevated substrate temperature. *Mater. Sci. Eng. B* 77, 110.
- Vasant Kumar, C.V.R., Mansingh, A., 1989. Effect of target-substrate distance on the growth and properties of RF-sputtered indium tin oxide films. *J. Appl. Phys.* 65, 1270.